NORSAR

ROYAL NORWEGIAN COUNCIL FOR SCIENTIFIC AND INDUSTRIAL RESEARCH

NORSAR Scientific Report No. 2–86/87

SEMIANNUAL TECHNICAL SUMMARY

1 October 1986 – 31 March 1987

L.B. Loughran (ed.)

Kjeller, May 1987

VII.3 Initial results from data analysis using the FINESA experimental small aperture array

This contribution describes initial research results obtained in conjunction with studies of data recorded by the FINESA experimental array in Finland, and compares these results to those previously obtained at NORESS.

The establishment of FINESA (Finnish Experimental Seismic Array) in late 1985 represents a joint undertaking between the University of Helskini (Institute of Seismology), Finland, and NTNF/NORSAR, Norway. All data and results from the array are openly available to the scientific community.

A comprehensive assessment of the capabilities of FINESA based on the first year of operation has been published by Korhonen et al (1987). The present contribution is essentially a synopsis of that paper, emphasizing features that are particularly relevant to the further development of the small-array concept first introduced with NORESS. The reader is referred to the referenced paper for details on the work described in the following. Copies are available, upon request, from either the University of Helsinki or NTNF/NORSAR.

Array deployment

The location of FINESA and the initial array geometry are shown in Fig. VII.3.1. The array is situated near the town of Heinola about 100 km northeast of Helsinki, and the distance to NORESS in Norway is approximately 800 km. FINESA comprises initially a total of 10 SPZ seismometers. The geometry consists of a 3-instrument ring (A1-A3) and a 6-instrument ring (B1-B6). In addition, one element (C1) lies outside these two rings. The maximum intersensor separation is about 1.5 km.

The A1 site also comprises two horizontal SP seismometers, thus providing a 3-component recording system within the array. The coordinates of the individual array sites are given in Table VII.3.1.

The geology of the siting area comprises precambrian gneissic rock, with little or no sedimentary overburden. It was in fact possible to place all seismometers in the initial deployment directly on outcropping rock. Topographically, the area is hilly, with the maximum height difference between sites being about 38 meters.

All 12 seismometers in FINESA are of type Geotech S-13. Data are transmitted in analog form by cables to the central recording site A1. The recorder is a Kinemetrics DDS-1105 system, which comprises 12 bits linear A/D converters, a radio receiver for time, a drum recorder (type Kinemetrics VR1) and a magnetic tape transport.

The FINESA system has been in operation since November 1985. Most of the time, the recording system has been operated in a trigger mode, using a built-in voting detector. This implies recording typically two minutes of data following each detection. The memory buffer of the Kinemetrics system is somewhat limited, but allows 3-4 seconds of noise data preceding each signal onset to be recorded for all channels.

The sampling rate is selectable, with a normal setting of 40 Hz. The anti-alias filter prior to A/D conversion has a high cutoff-frequency of 14.5 Hz. A calibration signal is inserted each time a new tape has been mounted, thus the first file of each tape is a calibration file.

Noise studies

For array sites, it is important to establish both the background noise level as a function of frequency and the noise correlation properties, since the gain that can be obtained by beamforming is largely

dependent on the structure of the noise. In the following we summarize our findings regarding ground motion spectra and noise correlation by distance for the FINESA array, and make comparisons with results for the NORESS array.

Ground motion spectra

In order to obtain an estimate of the ambient noise level at the site of the FINESA array, ground motion spectra were calculated for four time intervals. Two intervals were from November 1985, one during working hours and one during night time. Two intervals from October 1986 were chosen in the same way. For a direct comparison, ground motion spectra for data recorded at the NORESS array were calculated for the same four intervals. All noise spectra were estimated by the indirect covariance method described in Mykkeltveit et al (1985). This method gives the average properties of each noise interval, which in our computations were taken to be 100 seconds long. Each noise interval was visually inspected to ensure the absence of definite signal arrivals.

Fig. VII.3.2 shows ground motion spectra for two of the four intervals, for both FINESA and NORESS. These spectra, and other spectra shown in this report, have been corrected using the system response curves for the arrays.

Our studies so far indicate that for frequencies up to 2 Hz, the noise levels at FINESA and NORESS are comparable. At 1 Hz the noise level ranges between 2 and 20 nm^2/Hz for all noise samples. Between 0.5 and 2.0 Hz the falloff of the spectra is generally steep, ranging from 23 to 26 dB/octave for both sites. For both sites, there is a distinct change in the spectral slope at around 2.0 Hz. For frequencies above 2 Hz, however, the shapes of spectra at FINESA differ from those at NORESS, in particular during night time. Between 2.0 and 3.0 Hz the spectral slope has decreased to 7-10 dB/octave for FINESA and 11-13 dB/octave for NORESS. The four FINESA noise samples all show the same

general pattern and reach a minimum level of 42 to 46 dB below the 1 nm^2/Hz level when approaching the Nyquist frequency of 20 Hz.

Comparison of our results with those of Bungum et al (1985) and Tarvainen (1985) confirm that FINESA noise level at high frequencies is relatively high, compared to some other sites in Fennoscandia, but otherwise the results are in good agreement.

Noise correlation by distance

Both for NORESS and the provisional installations preceding its deployment in 1984, investigations into the correlation properties of the noise field played an important role in design and evaluation efforts. Curves showing intersensor correlation of the noise versus sensor separation can be directly utilized in predicting the signal-to-noise ratio gain that can be obtained by beamforming.

We have computed noise correlation curves for FINESA in the same way as has previously been done for NORESS (see Mykkeltveit et al, 1983; and Bungum et al, 1985). Altogether six noise intervals, each comprising 110 seconds of data, were subjected to correlation analysis in six frequency bands. For each of the frequency bands, the six average correlation curves were plotted on top of each other, and "envelopes" were formed that contained within them all six curves. The results for four of these bands are shown in Fig. VII.3.3, which for comparison also includes envelopes resulting from correlation analysis of noise recorded at NORESS.

All FINESA noise correlation curves show pronounced negative minima for the noise correlation. This feature has been shown to be compatible with a model of isotropic propagating noise near the Rayleigh wave velocity (Mykkeltveit et al, 1983). It has also been demonstrated that a signal-to-noise ratio gain beyond the standard $\sqrt{N}$ gain (N being

the number of sensors in the array) can be obtained by taking advantage of the negative correlation properties of the noise, and the "deeper" the negative minima, the larger the array gain.

The FINESA correlation curves appear to attain their minimum values at slightly smaller interstation distances, compared to the NORESS curves and also generally reach lower negative minima. More data analysis, however, is needed to firmly establish this conclusion. The possible implication is that an optimum array at the FINESA site would have a slightly smaller aperture than an optimum array at the NORESS site, and that such an array might have potential for a beamforming gain even exceeding that of NORESS.

Signal analysis

In order to demonstrate basic array signal processing techniques and also contribute towards an assessment of the potential of the FINESA miniarray, we have subjected signals from several regional and teleseismic events to detailed analysis. For comparison, NORESS data for two of the regional events were also analyzed, using the same algorithms. Analysis results from two regional events recorded at FINESA are shown in the following; otherwise, reference is made to Korhonen et al (1987).

Detailed analysis of a mining explosion

Fig. VII.3.4 (top) shows the FINESA data for the three-component station at site A1 for an event at 59.5°N, 28.5°E on December 27, 1985. There are two distinct P phases; the first arriving P phase is followed after about 1.2 s by a much stronger P phase. The dominant phase in the seismograms is the Lg (Sg) phase. We also see clear indications of the 1 Hz Rg phase in the Lg coda. In the bottom part of Fig. VII.3.4 we show the same three seismograms low pass filtered at 1 Hz, and the Rg waves stand out clearly.

Spectra for P, Lg and Rg for this event are shown in Fig. VII.3.5 along with a typical noise spectrum. The signal spectra are computed as described in Mykkeltveit et al (1985) and are based on data window lengths of 5 s for P and Lg and 20 s for Rg. We see that all phases have considerable energy above the noise level throughout the frequency band 1-20 Hz, but we must keep in mind the fact that the Lg signal window used contains high frequency P coda and likewise, the Rg window contains Lg coda arrivals.

Phase velocities and arrival azimuths were estimated using the wide-band frequency wavenumber (f-k) analysis technique described by Kværna and Doornbos (1986). Fig. VII.3.6 shows frequency-wavenumber spectra for two 1 s long time windows, with each window capturing the onset of a P arrival. Our analysis gives phase velocities that are in good agreement with results from refraction profiling experiments in Finland (e.g., Luosto et al, 1984), for the appropriate epicentral distance. The Lg and Rg phases were also subjected to wide-band f-k analysis and results are shown in Fig. VII.3.7. Again, the phase velocities are indeed as should be expected for these phases. We see that the estimated arrival azimuths are within 2 degrees of the true value (calculated from the network location) for all four phases.

NORESS data for a three component station for this mining explosion (epicentral distance now 954 km) are shown in Fig. VII.3.8 (top). There are three distinct phases: Pn, Sn and Lg. Spectra for these phases and the preceding noise are shown in the bottom part of Fig. VII.3.8. We see that in particular Pn, but also Sn, has energy well above the noise for frequencies up to 15-20 Hz. In comparing FINESA and NORESS P-wave spectra for this event, we see that there are similarities, and both spectra exhibit a pronounced peak at about 6 Hz.

Analysis of FINESA data for a Bothnian Bay earthquake

FINESA data for an earthquake that occurred in the Bothnian Bay on October 27, 1986 (magnitude m_D = 2.6, according to the Helsinki bulletin) are shown in Fig. VII.3.9. The epicentral distance from FINESA is 426 km. The phases Pn (very weak, just above the noise amplitude), Pg, Sn and Lg can be seen, and again, Lg is the overall dominant phase. Spectra for Pn, Sn and Lg, as well as the preceding noise are shown in Fig. VII.3.9 (bottom part). We observe that for Pn and Sn, the SNR is essentially constant over the frequency ranges 8-15 Hz and 4-15 Hz, respectively. The SNR may be constant over an even larger frequency range, but in analyzing these data we are limited by the 40 Hz sampling rate and the analog filter cut-off frequency of 14.5 Hz.

Wide-band f-k spectra were computed for the phases Pn, Sn and Lg and results are shown in Fig. VII.3.10. We see that again the resulting phase velocities are in agreement with the expectations, and there is also an indication that Sn has a slightly higher phase velocity than Lg. The derived azimuths are all a little on the high side of the "true" value of 323 degrees.

Event detection studies

In the initial mode of operation, the FINESA data acquisition system has been based on event recording using the built-in detector of the Kinemetrics DDS-1105. A detection is declared whenever the short-term to long-term signal ratio exceeds a predefined threshold on at least two out of three pre-selected channels.

This mode of operation has provided a considerable amount of event recordings for research purposes, but clearly does not provide a good measure of the inherent detection capability of the array. Therefore, we have also studied in detail continuous recordings over a shorter time period, using off-line processing with more advanced detection

algorithms. The results from this experiment are described in the following.

For the two-week period 21 Oct - 3 Nov 1986, the FINESA array was operated in the continuous recording mode. Because of the frequent tape changing necessary, the standard 40 Hz array data was recorded only during daytime, i.e., from about 0400 GMT to about 1800 GMT. For our purposes, this was quite adequate since the vast majority of reported regional events (quarry blasts) occur during daytime.

Detection analysis of the recorded "continuous" data was done using the RONAPP program (Mykkeltveit and Bungum, 1984) adapted to the FINESA configuration. Thresholds were set equal to those in use at NORESS and this resulted in a relatively large number of false alarms. Nevertheless, actual detections could be confidently identified by checking signal parameters such as SNR, frequency, estimated phase velocity and azimuth, and this was done by the analyst for the time period 21 -31 Oct.

The detections were then associated to the Helsinki regional bulletin. Considering only those bulletin events occurring when the FINESA system was in actual operation, we found that out of 68 reference events, 54 had at least one detected phase at FINESA, i.e., 84 per cent. This could be compared to the typical NORESS performance: For one year (1985) we found that NORESS reported at least one phase for 28 per cent of the events in the Helsinki regional bulletin (996 out of 3521). Thus, the advantage of being close to most epicenters outweighs by far the lower SNR gain in this case.

Both the P and S (or Lg) phases were detected for the majority of events. In addition, several Rg detections were made for events out to about 250 km epicentral distance.

In Fig. VII.3.11 the azimuths estimated for the P and S phases are plotted against true azimuth (derived from the Helsinki bulletin). The median (50%) error is about 5 degrees for both P and S, which is comparable to initial results reported for NORESS (Mykkeltveit and Ringdal, 1981). In that paper, the procedure later adopted for RONAPP was used, although time picks were made by the analyst rather than automatically.

Fig. VII.3.12 shows estimated phase velocities as a function of true azimuth for P and S phases, respectively. The line at 6 km/s is the separation line currently in use at NORESS, and it seems to provide quite good phase discrimination capabilities between primary and secondary phases also at FINESA. However, the separation is not 100 per cent, and there is a fair amount of scatter in the estimated velocities, even for events located close together. We consider that a somewhat larger array geometry will be necessary to obtain more stable phase velocity estimates, although broad-band estimation provides some improvements in this regard.

Conclusions

Noise characteristics: The seismic noise level at the FINESA site is slightly higher than that of NORESS at high frequencies (2-15 Hz) and comparable to that of NORESS in the 0-2 Hz band. This is consistent with previous observations for Fennoscandia. No particular noise sources have been identified in the vicinity of the array. The spatial noise correlation between sensors is very similar to that observed at NORESS; in particular the strong negative correlation at selected distance/frequency combinations is present also at FINESA, and appear to be even more pronounced than at NORESS.

Signal characteristics: The signal frequency contents at FINESA are comparable to those observed at NORESS, given similar epicentral distance. Signal correlation across the array is high, as expected,

except at very high frequencies. A noteworthy feature at FINESA is the presence of strong, coherent Rg waves (1 second period) for explosions out to more than 200 km distance. In contrast, NORESS does not observe Rg beyond 50-60 km.

Detection capability: The FINESA detection capability is excellent, both for regional and teleseismic phases. Our initial studies have indicated that with a sensitive RONAPP-type detector the array is capable of detecting more than 80 per cent of all regional events reported in the University of Helsinki Bulletin, in addition to a large number of events not included there. The detection capability is naturally somewhat lower when the built-in voting detector of the present Kinemetrics system is applied.

Phase characterization: The phase identification capability of the initial FINESA deployment has been evaluated using both single frequency and broadband f-k analysis. The estimated phase velocities are generally reliable indicators of phase type (primary or secondary), although the separation is not 100 per cent. The resolution is not sufficient to separate Sn from Lg on phase velocity alone, a result also found at NORESS. Azimuth estimates are sufficiently accurate for successful phase association; median error was found to be about 5 degrees both for P and S, using automatic, single frequency f-k estimation.

One of the main achievements of the FINESA study has been to demonstrate that many of the processing techniques that have contributed to the outstanding performance of NORESS can be successfully applied also at other sites in Fennoscandia. This opens up for the

possibility of significantly improved capabilities when applying data from several regional arrays in a future multi-array processing scheme.

F. Ringdal
S. Mykkeltveit
T. Kværna
P.W. Larsen
R. Paulsen
H. Korhonen, Univ. of Helsinki
S. Pirhonen, Univ. of Helsinki

REFERENCES

Bungum, H., S. Mykkeltveit & T. Kværna (1985): Seismic noise in Fennoscandia, with emphasis on high frequencies, Bull. Seism. Soc. Am., 75, 1489-1514.

Korhonen, H., S. Pirhonen, F. Ringdal, S. Mykkeltveit, T. Kværna, P.W. Larsen and R. Paulsen (1987): The Finesa array and preliminary results of data analysis, Univ. of Helsinki, Inst. of Seismology.

Kværna, T. & D.J. Doornbos (1986): An integrated approach to slowness analysis with arrays and three-component stations. In: NORSAR Semiannual Technical Summary, 1 Oct 85 - 31 Mar 86 (L.B. Loughran, ed.), NORSAR, Kjeller, Norway.

Luosto, U., E. Lanne, H. Korhonen, A. Guterch, M. Grad, R. Materzok & E. Perchuc (1984): Deep structure of the earth's crust on the SVEKA profile in central Finland. Annales Geophys. 2, 559-570.

Mykkeltveit, S. & H. Bungum (1984): Processing of regional seismic events using data from small-aperture arrays. Bull. Seism. Soc. Am., 74, 2313-2333.

Mykkeltveit, S. & F. Ringdal (1981): Phase identification and event location at regional distances using small-aperture array data. In: Identification of Seismic Sources - Earthquake or Underground Explosion (E.S. Husebye & S. Mykkeltveit, eds.), D. Reidel Publ. Co., Dordrecht, The Netherlands.

Mykkeltveit, S., K. Åstebøl, D.J. Doornbos & E.S. Husebye (1983): Seismic array configuration optimization. Bull. Seism. Soc. Am., 73, 173-186.

Mykkeltveit, S., D.B. Harris & T. Kværna (1985): Preliminary evaluation of the event detection and location capability of the small-aperture NORESS array. In: NORSAR Semiannual Technical Summary 1 Oct 84 - 31 Mar 85 (L.B. Loughran, ed.), NORSAR, Kjeller, Norway.

Tarvainen, M. (1985): Results of noise studies in Finland 1981-1984, Report No. T-30, Inst. of Seismology, Univ. of Helsinki.

Station Code	Latitude (°N)	Longitude (°E)	Altitude (m)
ALNS	61.4444389	26.0793387	137.92
ALZ	61.4444439	26.0793270	137.86
ALEW	61.4444462	26.0793442	137.92
A2	61.4412337	26.0736561	161.60
A3	61.4447211	26.0715517	153.43
B1	61.4422706	26.0844928	164.98
B2	61.4390893	26.0984178	158.69
B3	61.4394023	26.0705952	175.57
B4	61.4435798	26.0650265	157.84
B5	61.4466901	26.0710893	142.68
B6	61.4469378	26.0808177	146.85
C1	61.4384113	26.0595485	157.69

Accuracy internal: 0.1 m
" global: approx. 10 m

Table VII.3.1 FINESA seismometer coordinates.

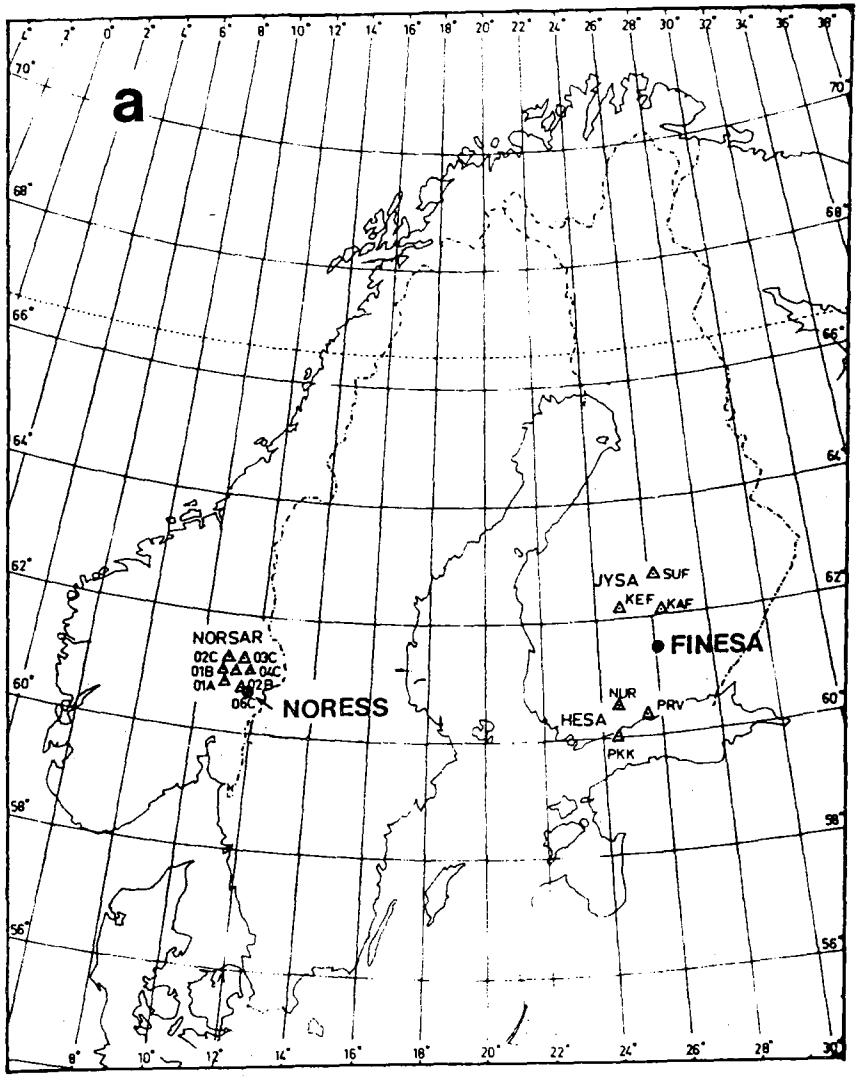

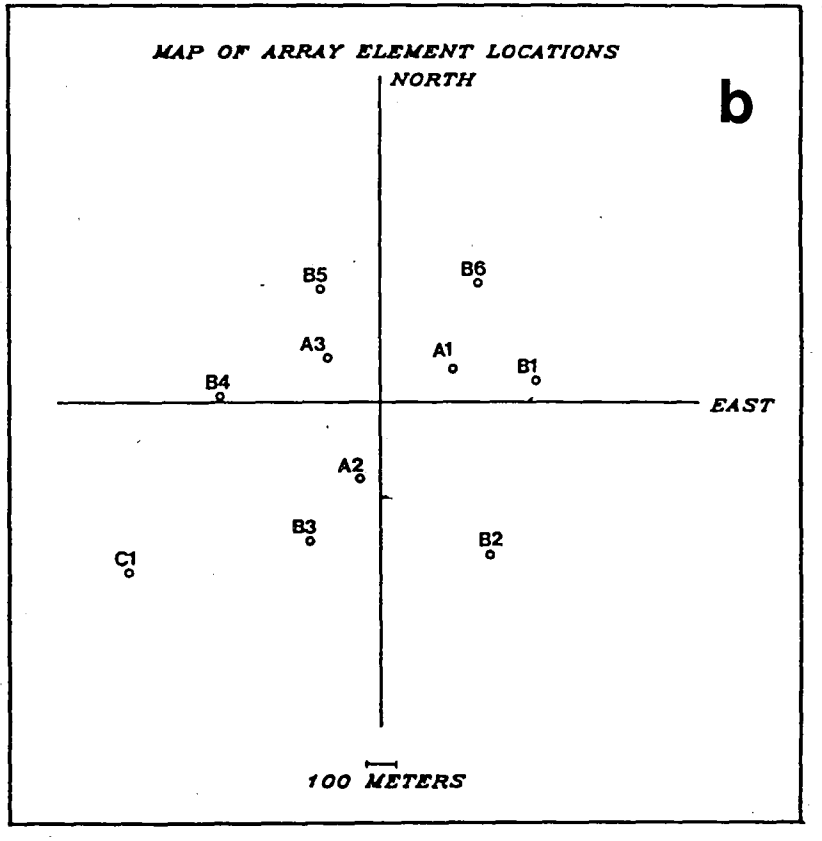

Fig. VII.3.1 (a) A map of Fennoscandia showing the locations of NORESS and FINESA relative to other seismic arrays in Norway and Finland. (b) The initial FINESA geometry is also shown. The central recording equipment is at site A1, which also comprises a three-component short period seismometer system. All other sites contain vertical SP seismometers only.

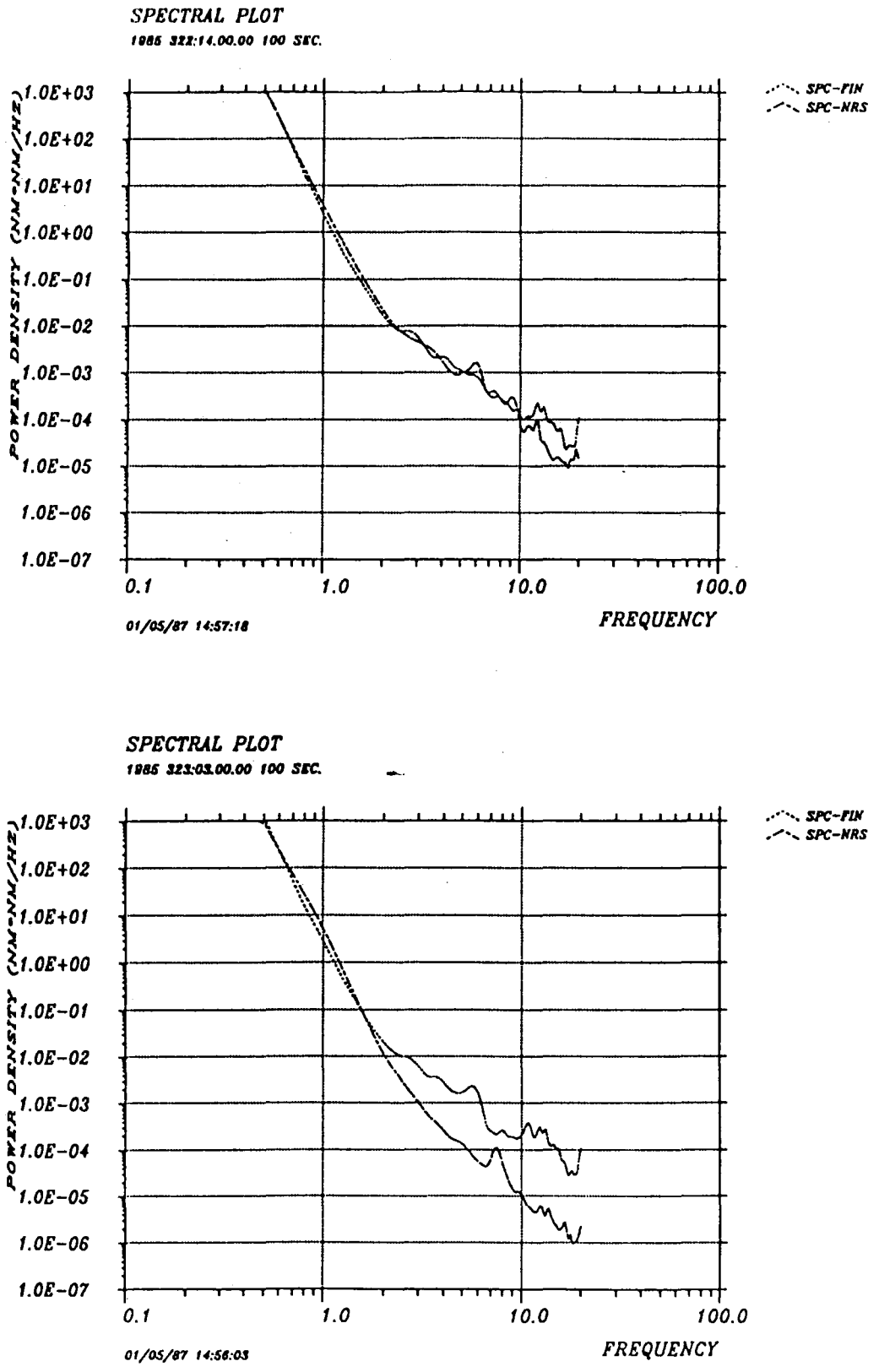

Fig. VII.3.2 FINESA and NORESS ground motion spectra for day 322, 1400 GMT (top) and day 323, 0300 GMT (bottom) of 1985. The FINESA noise spectra are given by dotted lines, whereas the curves for NORESS are dashed-dotted.

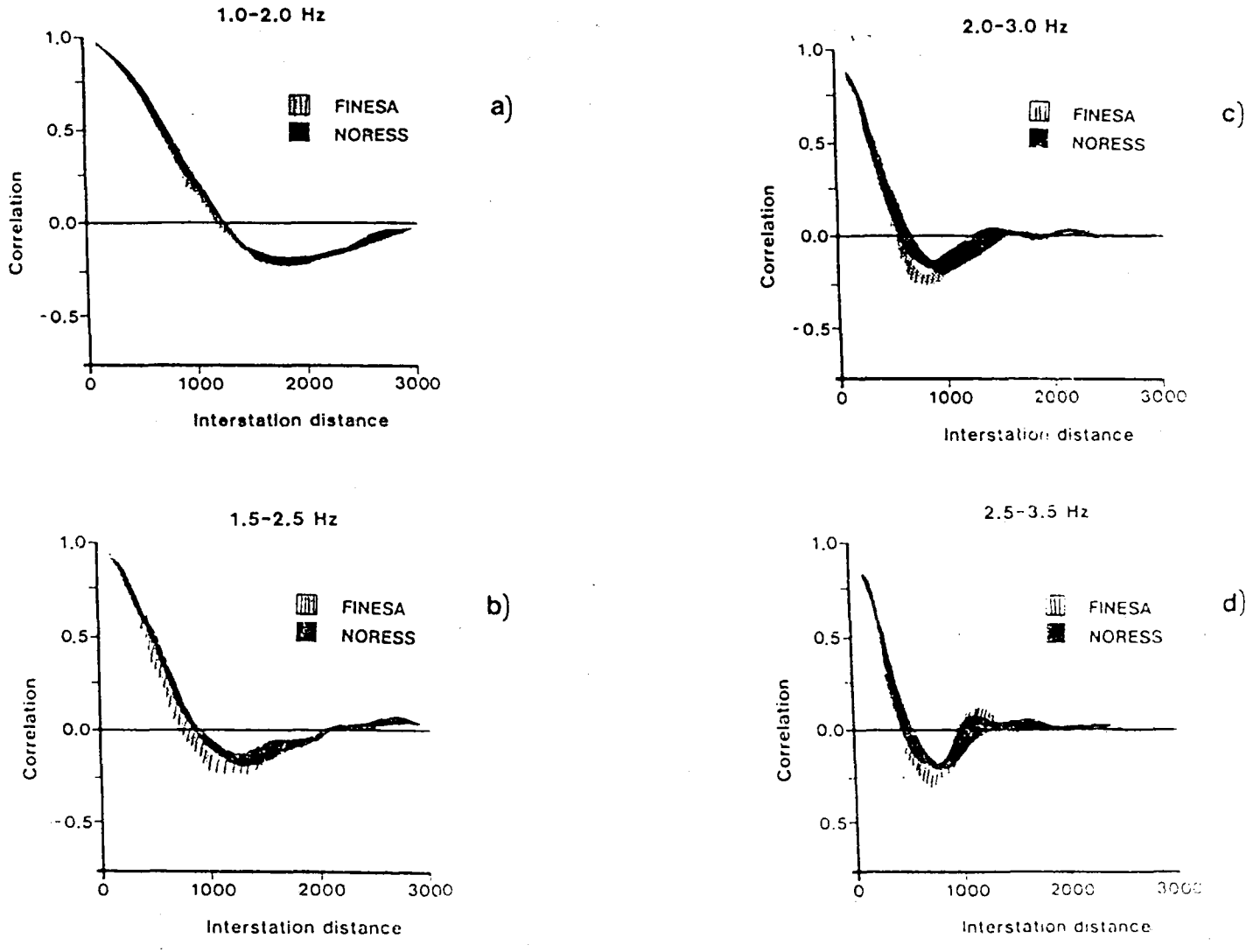

Fig. VII.3.3 Average noise correlations (see text) for four frequency bands for the FINESA and NORESS arrays.

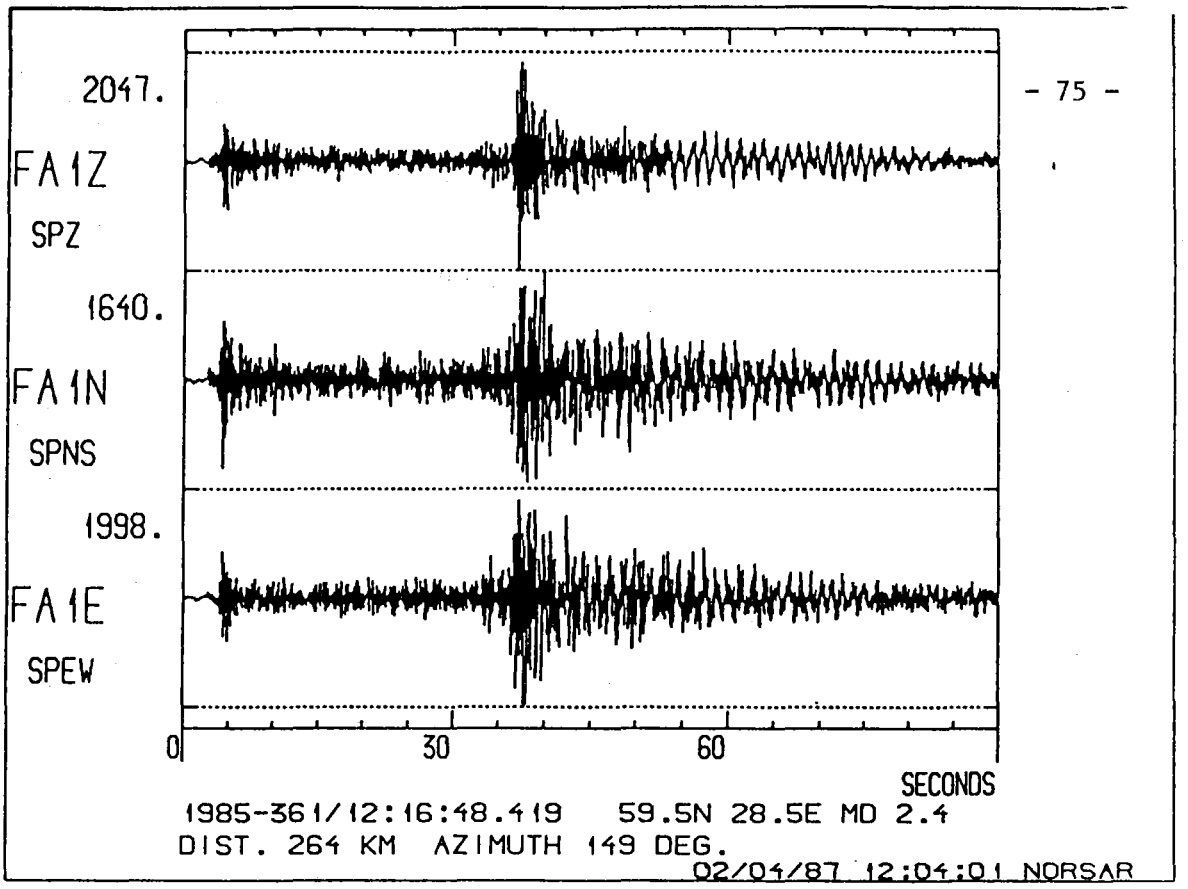

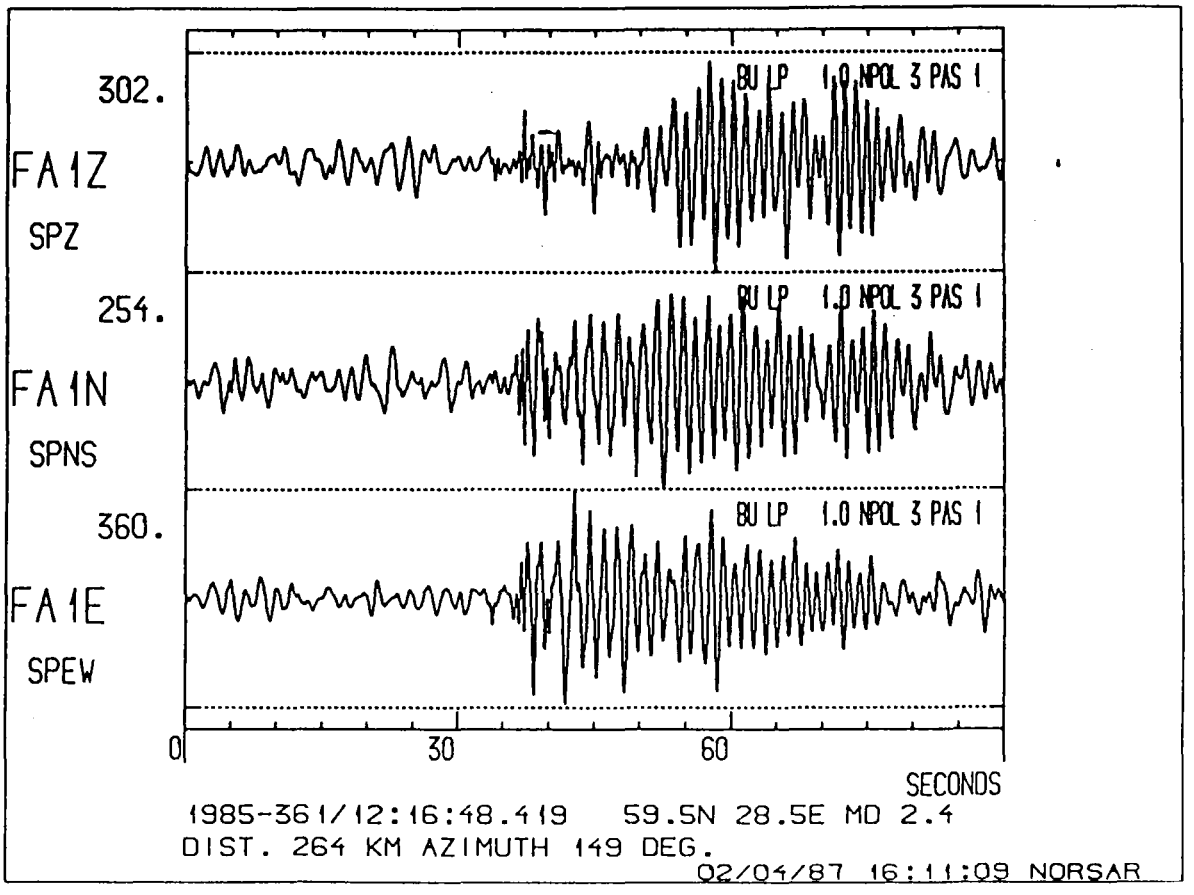

Fig. VII.3.4 FINESA data for a mining explosion (top) and the same data low pass filtered at 1 Hz (bottom). Distance and azimuth given on the plots are according to the epicenter determination by the network of the University of Helsinki.

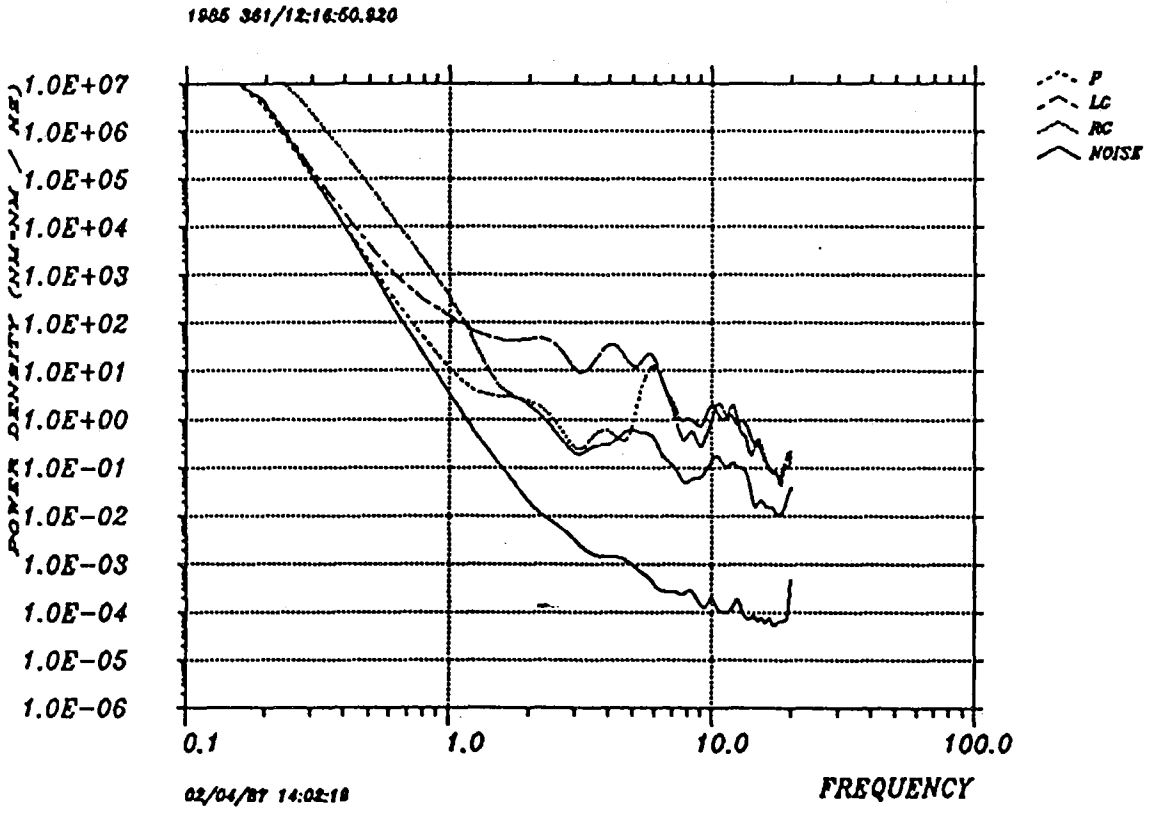

Fig. VII.3.5 Spectra for the phases P, Lg and Rg and noise, for data shown in Fig. VII.3.4.

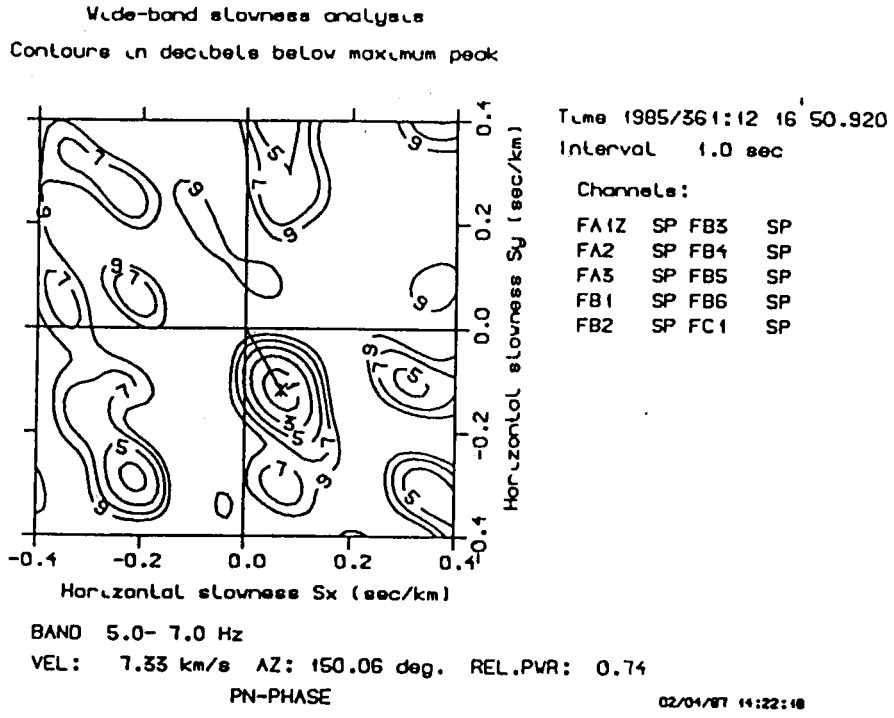

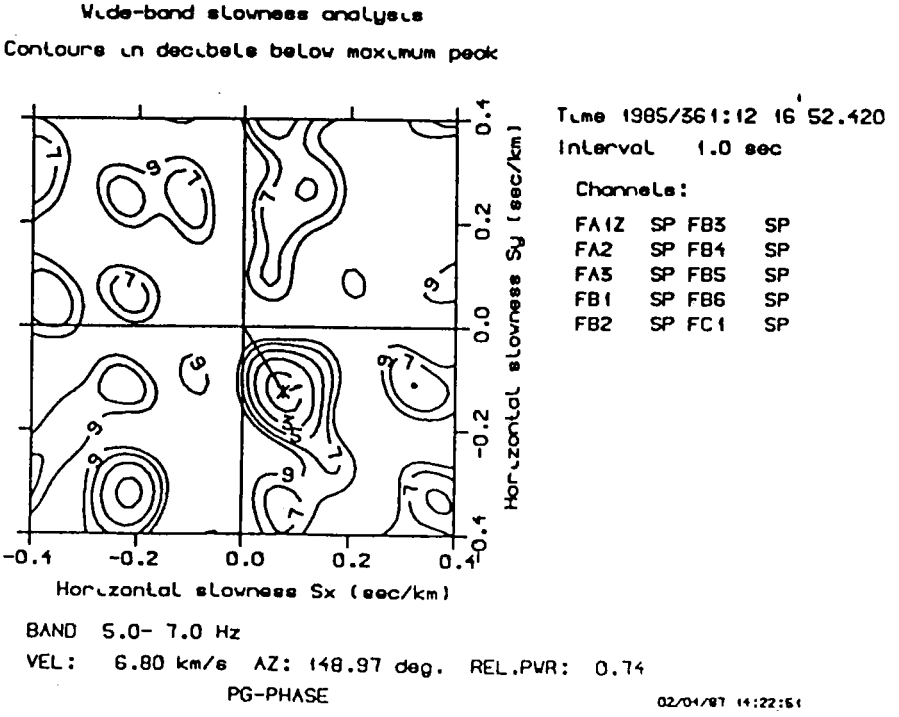

Fig. VII.3.6 Wide-band f-k spectra for the first arriving P phase (top) and the following strong P phase (bottom) of the event in Fig. VII.3.4.

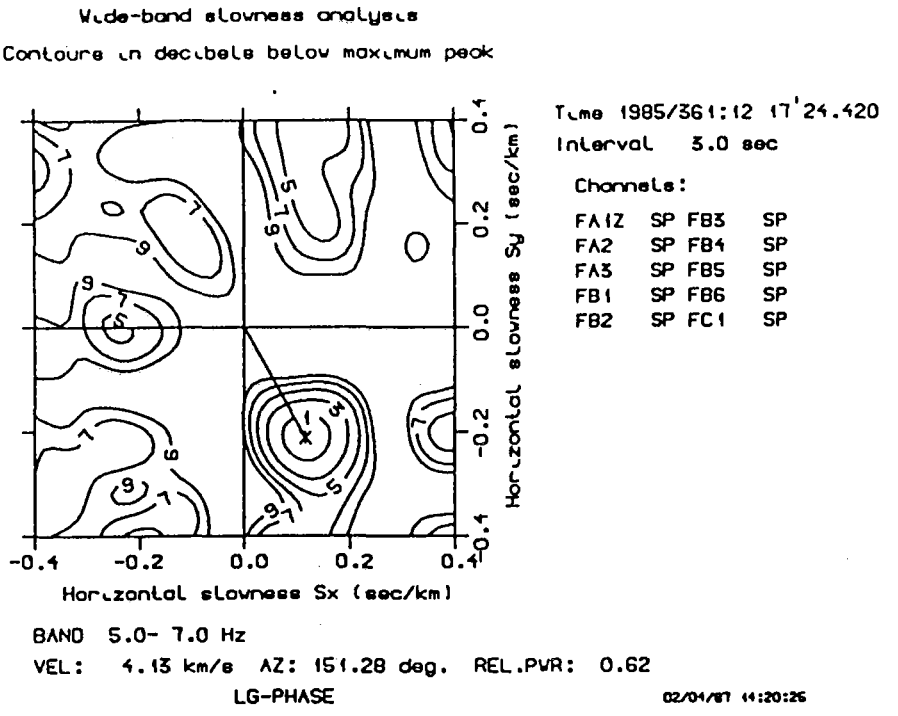

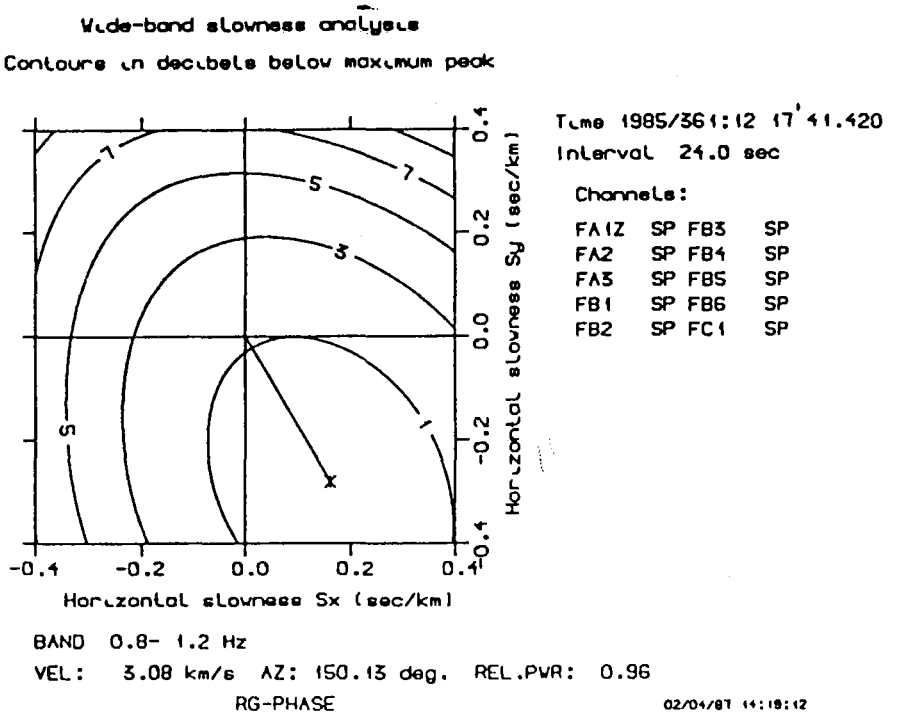

Fig. VII.3.7 Wide-band f-k spectra for the Lg phase (top) and Rg phase (bottom) of the event in Fig. VII.3.4.

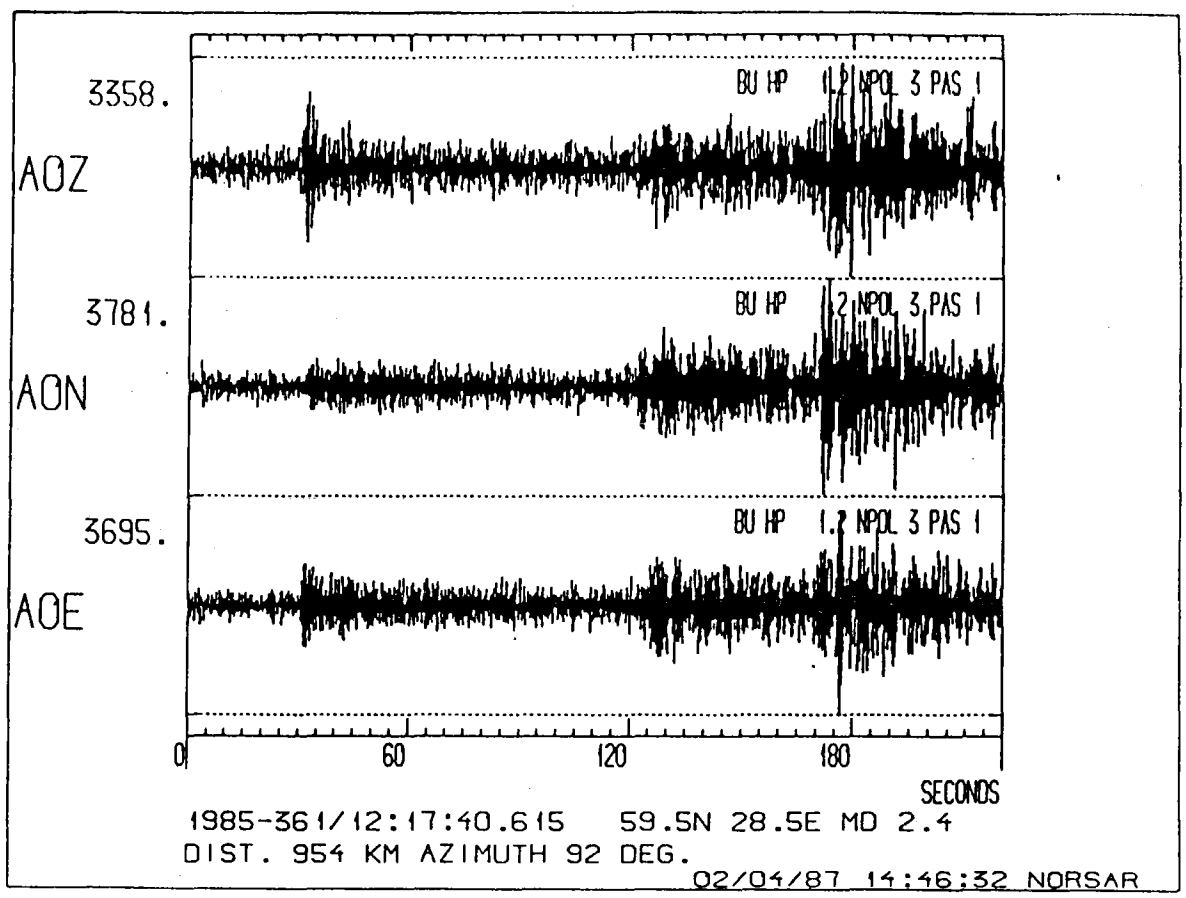

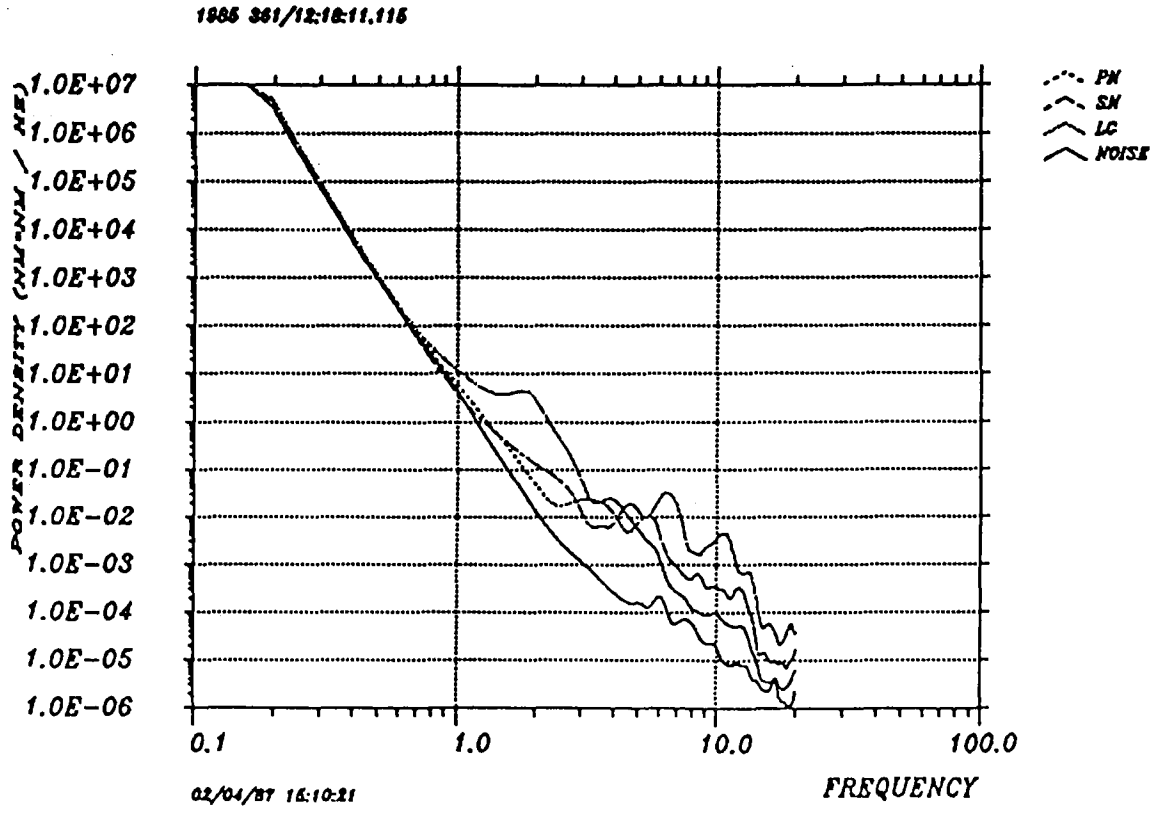

Fig. VII.3.8 NORESS data for the mining explosion (top) with spectra (bottom).

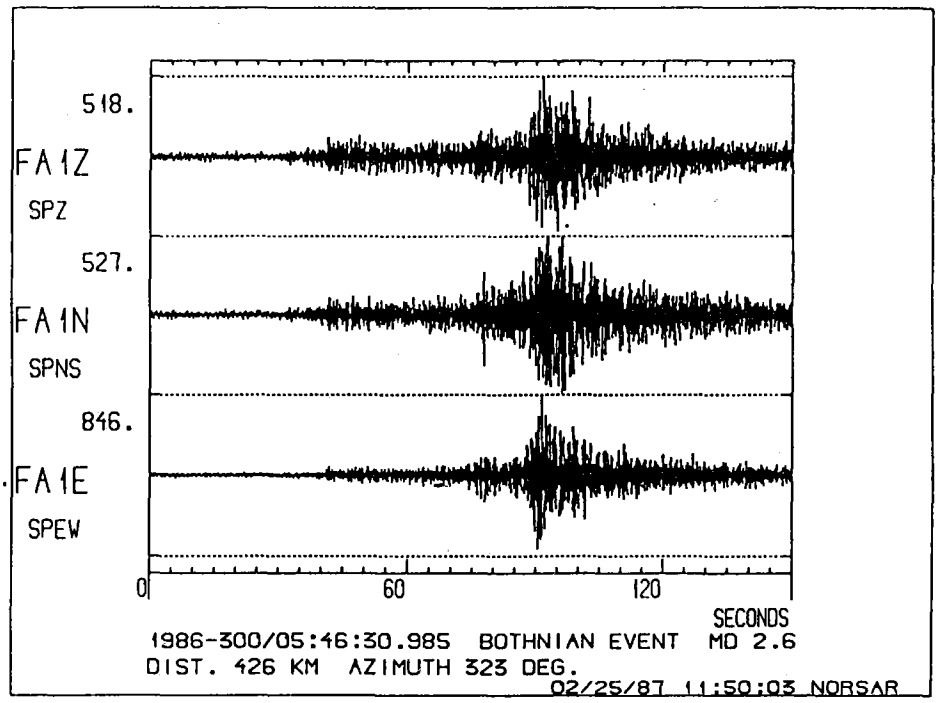

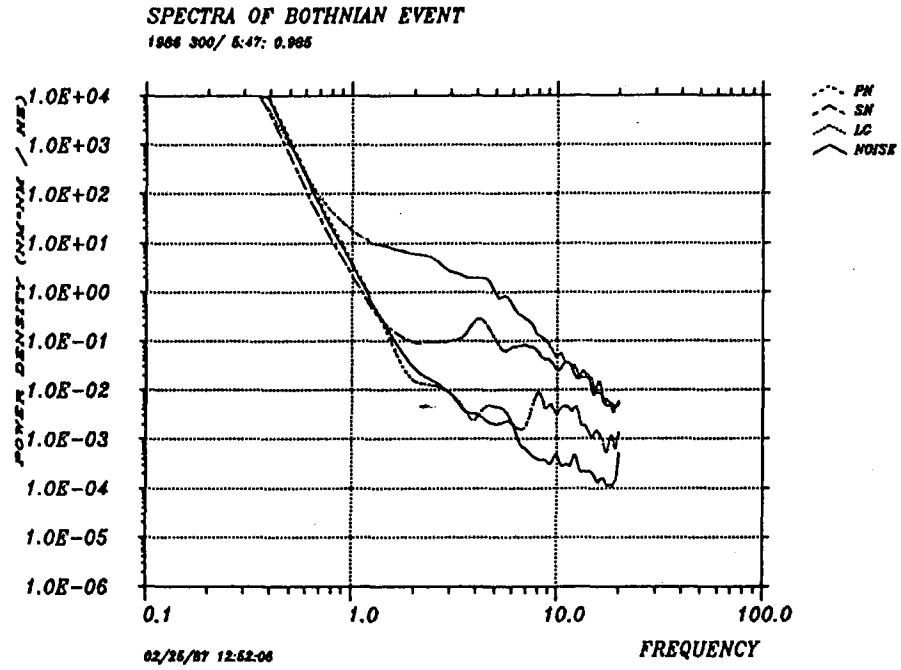

Fig. VII.3.9 FINESA three-component station data for a Bothnian Bay earthquake on October 27, 1986 (top). Spectra for the phases Pn, Sn and Lg for the event together with a spectrum of the preceding noise are shown at the bottom.

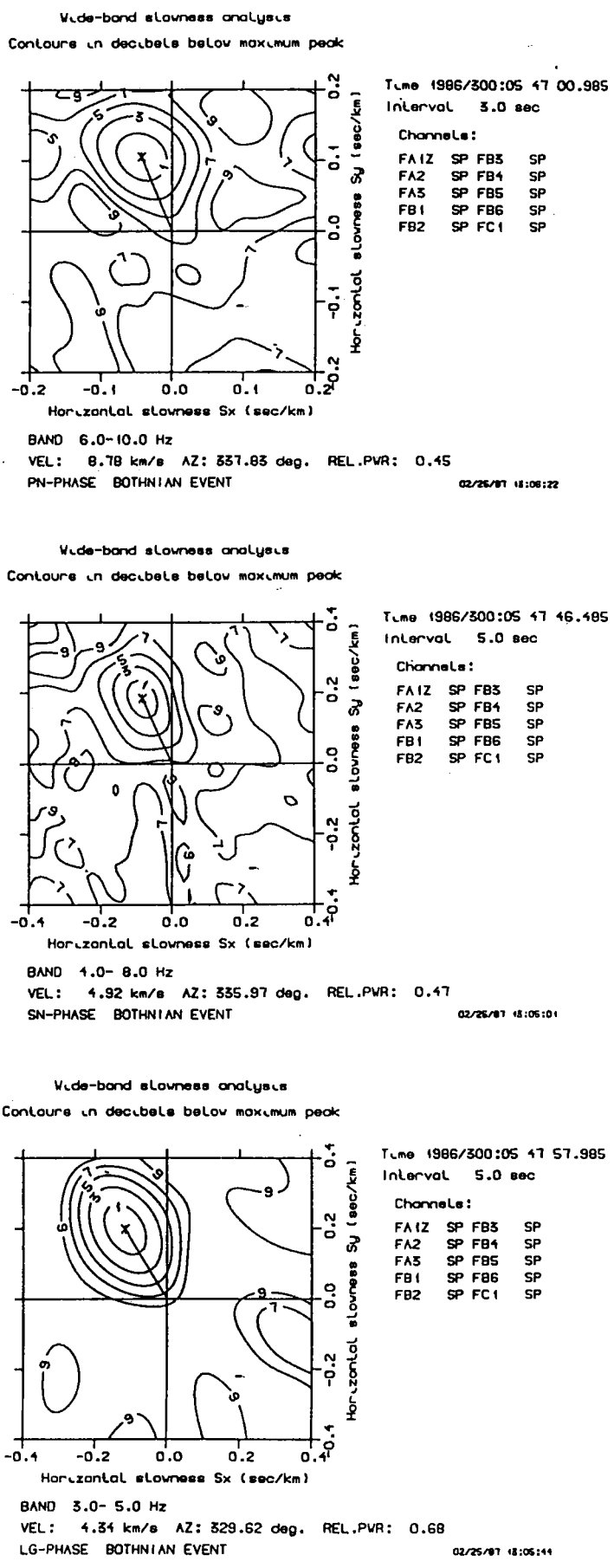

Fig. VII.3.10 Wide-band f-k spectrum for the Pn, Sn and Lg phases of the event in Fig. VII.3.9.

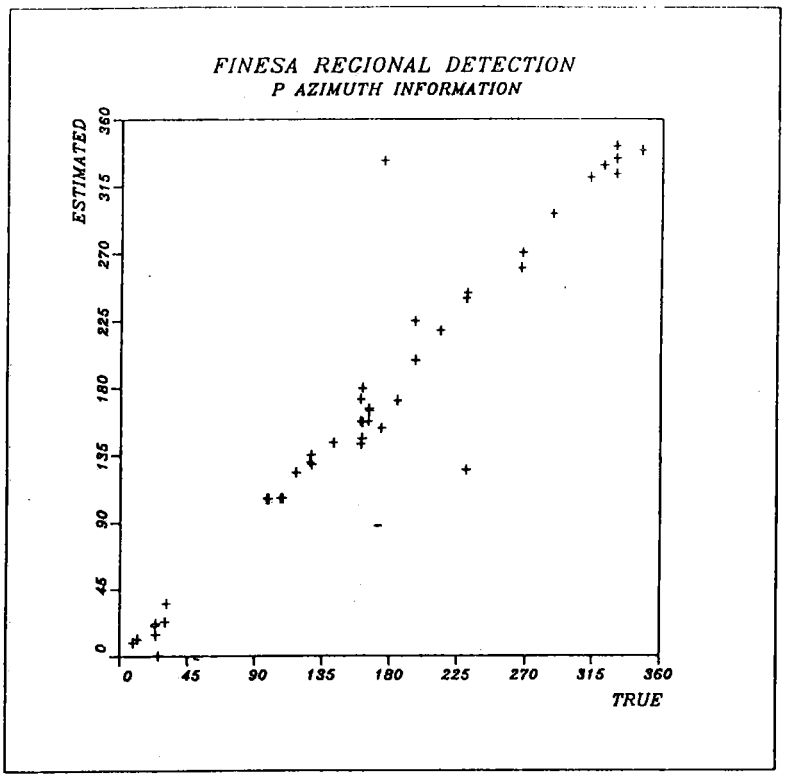

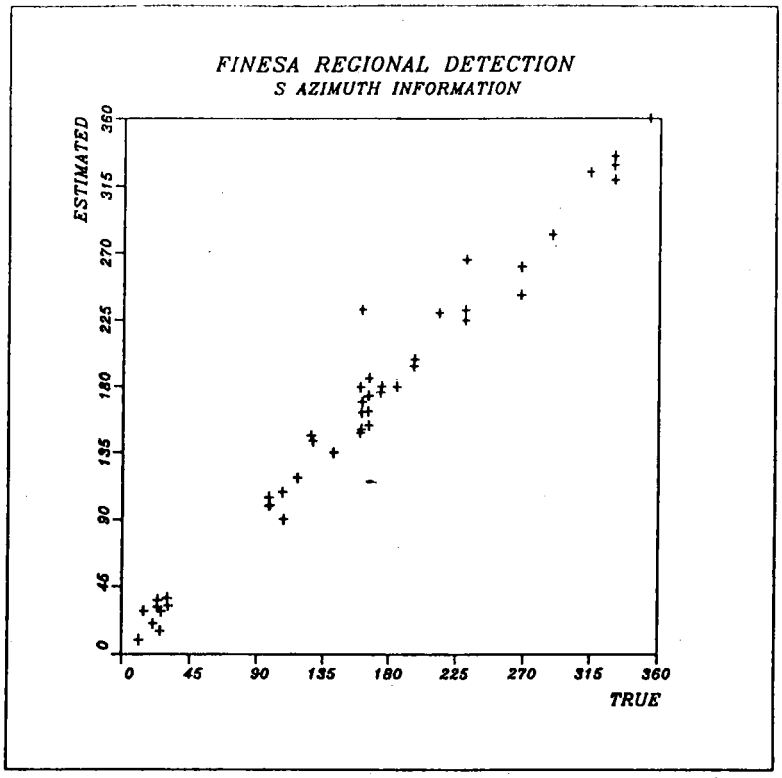

Fig. VII.3.11 Estimated versus true azimuth plotted for detected P and S phases.

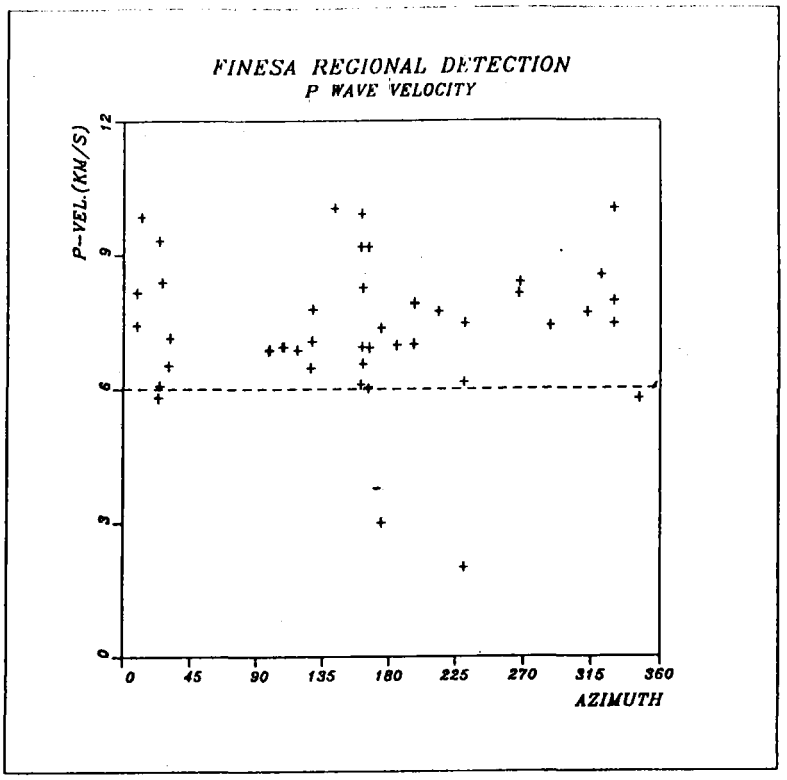

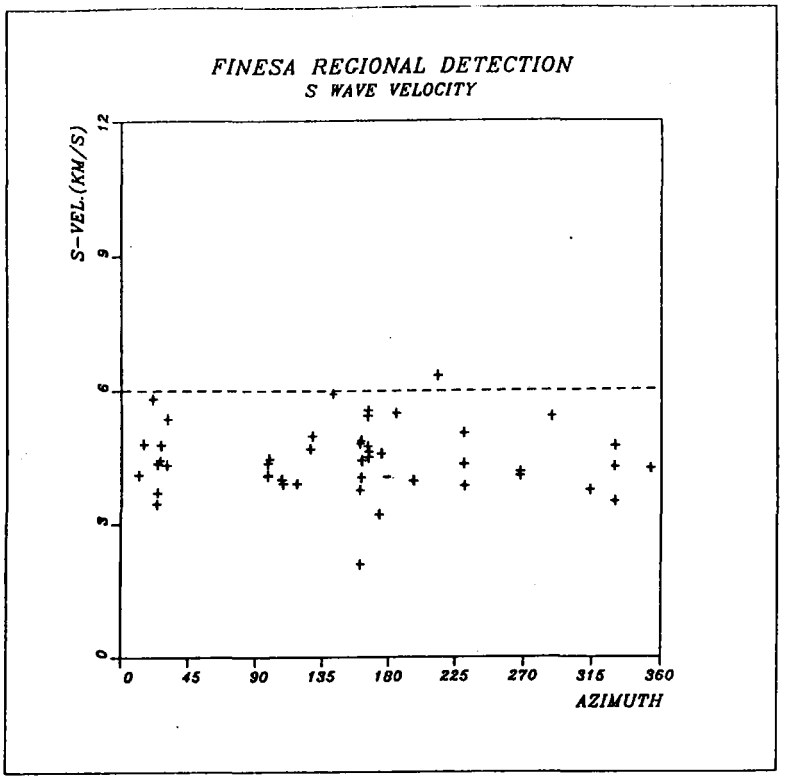

Fig. VII.3.12 Estimated phase velocity plotted versus true azimuth for detected P and S phases.